Studies on the Mechanism of Inactivation of the HIV-1 Nucleocapsid Protein NCp7 with 2-Mercaptobenzamide Thioesters

Lisa M. Miller Jenkins,[†] J. Calvin Byrd,[†] Toshiaki Hara,[‡] Pratibha Srivastava,[‡] Sharlyn J. Mazur,[‡] Stephen J. Stahl,[§] John K. Inman,[∥] Ettore Appella,[‡] James G. Omichinski,*[†,⊥] and Pascale Legault*[,†]

Department of Biochemistry and Molecular Biology, University of Georgia, Athens, Georgia 30602, Laboratory of Cell Biology, NCI, National Institutes of Health, Bethesda, Maryland 20892, Protein Expression Laboratory, National Institute of Arthritis, Musculoskeletal, and Skin Diseases, National Institutes of Health, Bethesda, Maryland 20892, Laboratory of Immunology, NIAID, National Institutes of Health, Bethesda, Maryland 20892, and Department of Chemistry, University of Georgia, Athens, Georgia 30602

Received September 24, 2004

The HIV-1 nucleocapsid protein (NCp7) is a small basic protein with two CysCysHisCys zinc-binding domains that specifically recognizes the Ψ-site of the viral RNA. NCp7 plays a number of crucial roles in the viral lifecycle, including reverse transcription and RNA encapsidation. Several classes of potential anti-HIV compounds have been designed to inactivate NCp7 through zinc ejection, including a special class of thioester compounds. We have investigated the mechanism of action of two N-substituted-*S*-acyl-2-mercaptobenzamide compounds (compounds **1** and **2**) that target NCp7. UV/Visible spectroscopy studies demonstrated that both thioesters were able to eject metal from NCp7. NMR and mass spectroscopy studies showed that the thioester compounds specifically ejected zinc from the carboxyl-terminal zinc-binding domain of NCp7 by covalent modification of Cys_{39}. Exposure of NCp7 to compounds **1** and **2** destroyed its ability to specifically bind RNA, whereas NCp7 already bound to RNA was protected from zinc ejection by the thioesters. The thiol component of the thioesters (compound **3**, 2-mercaptobenzoyl-*β*-alaninamide) did not eject zinc from NCp7, but when compound **3** was incubated with acetyl CoA prior to incubation with NCp7, we observed extensive metal ejection. Thus, the thiol released by the reaction of compounds **1** and **2** could be re-acylated in vivo by acyl CoA to form a new thioester compound that is able to react with NCp7. These studies provide a better understanding of the mechanism of action of thioester compounds, which is important for future design of anti-HIV-1 compounds that target NCp7.

Introduction

HIV-1 infection afflicts millions of people worldwide, killing three million people in the last year alone (www.unaids.org). Though much work has been done to stop the progression of HIV-1 infection to AIDS, several issues remain. Traditional combination therapies do not completely eradicate the virus. Consequently, long-term treatment is required, which is complicated by problems of patient compliance and metabolic side effects.[1−4] Over the long course of combination therapy, drug-resistant strains of HIV-1 often arise. These resistant strains necessitate the continual development of new antiviral drugs.

One potential target for antiviral therapy is the HIV-1 nucleocapsid protein (NCp7). NCp7 plays many crucial roles throughout the retrovirus lifecycle as a general nucleic acid binding protein. During reverse transcription, NCp7 facilitates binding of the $tRNA_3^{Lys}$ to the primer binding site and promotes strand annealing.[5−7] In addition, NCp7 enhances the integration of viral DNA into the host chromosome.[8,9] It is also essential for dimerization and packaging of full-length viral RNA into the new virions.[10−12]

NCp7 is a small basic protein that contains two zinc-binding domains (ZD1 and ZD2). The two zinc-binding domains each chelate one zinc ion using three cysteine and one histidine residues as ligands (Figure 1A). NMR solution studies of NCp7 show that in the free protein, the two zinc-binding domains form small globular structures, whereas the amino and carboxyl termini of the protein are disordered.[13−15] The zinc-binding domains and several basic amino acids at the amino terminus of NCp7 are required for sequence-specific RNA binding. The structure of the zinc-binding domains and the mutationally nonpermissive nature of NCp7 suggest that HIV-1 strains resistant to drugs targeted against this protein are unlikely to develop.[10,16−19]

Over the last several years, numerous studies have been reported on compounds that were designed to inhibit NCp7. Most of the compounds eject zinc from NCp7 (zinc ejectors), destroying the structure of the protein and preventing it from functioning. The first zinc ejector was 3-nitrosobenzamide (NOBA), which showed inhibition of HIV-1 replication, but was highly reactive, and thus toxic.[20] Compounds of this type lacked selectivity, as they reacted indiscriminately with both zinc-binding domains of NCp7 as well as with other zinc-

* Corresponding authors. Present address: Université de Montréal, Département de Biochimie, C. P. 6128, Succursale Centre-Ville, Montréal, QC H3C 3J7, Canada. Phone: (514) 343-7326. Fax: (514) 343-2210. E-mail: pascale.legault@umontreal.ca, jg.omichinski@umontreal.ca.

[†] Department of Biochemistry and Molecular Biology, University of Georgia.

[‡] Laboratory of Cell Biology, NCI.

[§] Protein Expression Laboratory, National Institute of Arthritis.

[∥] Laboratory of Immunology, NIAID.

[⊥] Department of Chemistry, University of Georgia.

10.1021/jm0492195 CCC: $30.25
Published on Web 03/25/2005

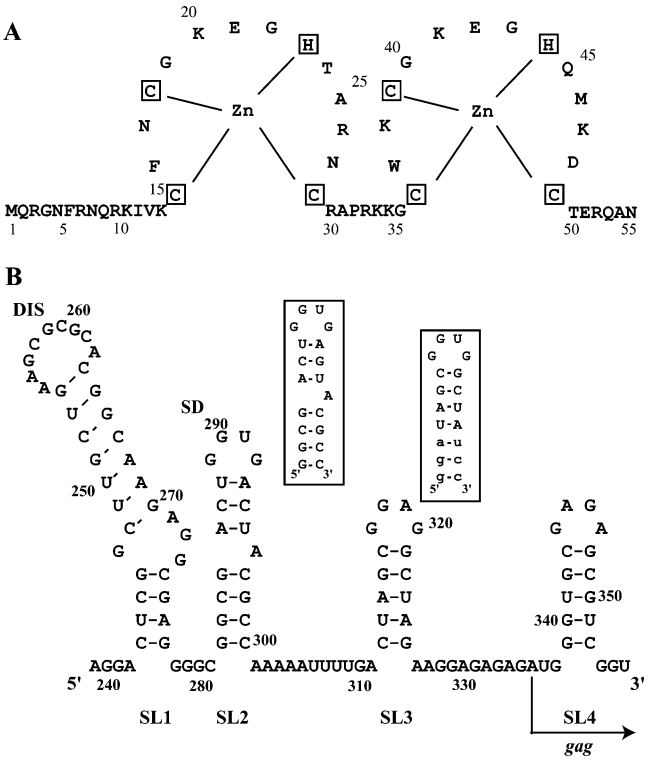

Figure 1. (A) Amino acid sequence of NCp7 used in this study, showing the zinc-coordinating residues highlighted in boxes. (B) Nucleotide sequence and secondary structure of the HIV-1 Ψ-site. Boxed sequences correspond to the sequences of the ΨSL2 and ΨSL3 RNAs used in this study. Nucleotides in lower case are nonnatural residues added for improved in vitro transcription by T7 RNA polymerase.

binding domains present in cellular proteins. Further studies led to the development of less toxic and more selective compounds, such as the disulfide benzamide (DIBA) and azodicarbonamide (ADA) compounds.[21,22] Both the DIBA and ADA compounds inhibit HIV-1 replication and show a degree of specificity for NCp7. For example, the carboxyl-terminal zinc-binding domain (ZD2) of NCp7 was found to be more reactive with the DIBA compounds than the amino-terminal zinc-binding domain (ZD1).[23] In addition, the DIBA compounds did not inhibit the functional activity of cellular proteins containing zinc-binding domains, including the poly-(ADP ribose) polymerase and the Sp1 and GATA-1 transcription factors.[24] Mass spectrometry demonstrated that both Cys_{36} and Cys_{49} of ZD2 were covalently modified by the DIBA compounds.[23] Despite their selectivity, the DIBA compounds had the disadvantage that they contained an easily reduced disulfide bond that severely limited the half-life of the compound.[25]

Among the most recent class of zinc ejectors to be developed are the pyridinioalkanoyl thioesters.[26] These thioester compounds have high antiviral activity and low cellular toxicity. They are water soluble and have been shown to eject zinc from NCp7.[26,27] Initial studies demonstrated that silver ions had to be added to the reaction in vitro to "activate" the thioester compounds; no zinc ejection was observed with either silver ions alone or the thioester compounds alone.[28] Mass spectrometry revealed that these thioester compounds selectively modified NCp7 in ZD2 as was seen with the DIBA compounds.[28] These thioester compounds were

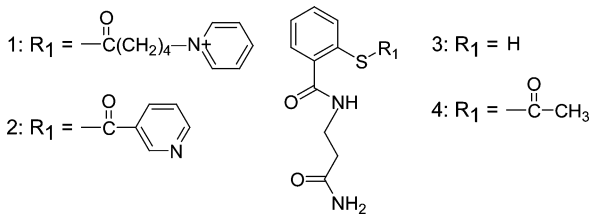

Figure 2. Chemical structure of thioester compounds and derivatives used in this study.

also shown to have no effect on DNA binding by Sp1, suggesting that they might not target other zinc-binding domains in cellular proteins.[26] Recently, the in vivo antiviral activity of two *S*-acyl-2-mercaptobenzamide thioesters (Figure 2, compounds **1** and **2**) was described.[29] These compounds were shown to have antiviral activity in a murine model.[29] Orally administered compound **2** actually evoked an antiviral response similar to that of the protease inhibitor indinavir.[29] Though it is postulated that these new thioester compounds have antiviral activity because they eject zinc from NCp7, the exact mechanism of zinc ejection has not been established. Understanding how these thioester compounds function should be very useful for the design of improved compounds to target NCp7.

Here, we have used UV/visible spectroscopy to evaluate the ability of the thioester compounds **1** and **2** to eject metal from purified, recombinant NCp7. NMR spectroscopy and mass spectrometry were used to study the structural interaction between the thioester compounds and NCp7, as well as to determine if these compounds covalently modify NCp7 and to identify any reaction products. Finally, we used gel mobility shift assay to study the ability of the thioester compounds to disrupt NCp7's function as an RNA-binding protein. These studies provide a better understanding of the mechanism of action of thioester compounds.

Experimental Section

Synthesis of Compounds. The preparation of compound **1** (*N*-[2-(5-pyridiniovaleroylthio) benzoyl]-β-alaninamide bromide) and compound **3** (N^{β}-(2-mercaptobenzoyl)-β-alaninamide) (Figure 2) were carried out as previously described.[30] Compound **2** (*N*-[2-(nicotinoylthio)benzoyl]-β-alaninamide hydrochloride) was synthesized as outlined.[26,30] The uncharged compound **2** was prepared as described.[31] Compound **4** (*N*-[2-acetylthiobenzoyl]-β-alaninamide) (Figure 2) was synthesized as described.[31] Compound **3** and the thioester compounds were lyophilized in 500 μL aliquots at a concentration of 1 mM and stored at −20 °C.

Sample Preparation. The coding sequence for HIV-1 NCp7 (HXB2 isolate) was cloned into the *Escherichia coli* vector pET11a and expressed in host strain Rosetta (DE3) (Novagen, WI). Uniformly ^{15}N-labeled or ^{13}C/^{15}N-labeled NCp7 was obtained by growing the cells in modified minimal media containing ^{15}N-labeled (>98%) ammonium chloride and/or ^{13}C-labeled (>99%) glucose as the sole nitrogen and carbon sources, respectively. Cells were grown overnight at 37 °C, and protein expression was induced for 4 h with 0.66 mM or 1 mM isopropyl-β-D-thiogalactopyranoside (IPTG) for cultures grown in minimal media or Luria Broth, respectively. The cells were pelleted and resuspended in 25 mM Tris pH 8.0, 1 mM EDTA, 2 mM dithiothreitol (DTT), 6 mM benzamidine. The cells were then lysed by French press and centrifuged at 100 000*g* for 45 min. The supernatant was applied to a DEAE-Sepharose Fast Flow (Amersham Biosciences, NJ) column (300 mL bed volume), equilibrated with Buffer A (25 mM Tris pH 8.0, 1 mM EDTA, 2 mM DTT), and eluted using a gradient (0−100%

B over 1500 mL) of Buffer B (25 mM Tris pH 8.0, 1 mM EDTA, 2 mM DTT, 1 M NaCl). The pooled NCp7 fractions were then applied to a SP-Sepharose Fast Flow (Amersham Biosciences, NJ) column (300 mL bed volume), equilibrated with Buffer A and eluted using a gradient (0−100% B over 1500 mL) of Buffer B. The fractions containing NCp7 were pooled and purified on a C-8 reverse phase (Vydac) high-performance liquid chromatography (HPLC) column using a gradient of 10−30% acetonitrile in 0.05% aqueous trifluoroacetic acid (TFA). The purified NCp7 was flash frozen and lyophilized.

Purified NCp7 was refolded using the following procedure. Lyophilized protein was first resuspended at a concentration of ∼0.2 mM in 0.05% TFA. Five equivalents of $ZnCl_2$ (zinc-refolded NCp7) or $CoCl_2$ (cobalt-refolded NCp7) were then added to the NCp7 solution as 50 mM metal solutions in 0.05% TFA. The solution was slowly titrated to pH 6.0 with 0.2 M NaOH. The zinc-refolded NCp7 was flash frozen and lyophilized. Prior to use, zinc-refolded NCp7 (1 mM) was resuspended in NMR buffer A (20 mM sodium phosphate pH 7.0) in 90% H_2O/10% D_2O. The buffer of the cobalt-refolded NCp7 was adjusted to 20 mM sodium phosphate pH 7.0. The cobalt-refolded NCp7 was used immediately after refolding.

ΨSL2 and ΨSL3 RNAs (Figure 1B) were transcribed in vitro using T7 RNA polymerase, synthetic oligonucleotide templates, and nucleoside triphosphates. The T7 RNA polymerase was purified based upon a published procedure.[32] The RNAs were purified to single-nucleotide resolution by 20% denaturing polyacrylamide gel electrophoresis. Each RNA was further purified by DEAE-Sephacel chromatography (Amersham Biosciences, NJ). The ΨSL2 and ΨSL3 RNAs were concentrated with an Amicon Centricon-3 concentrator (Millipore, MA) and exchanged into NMR buffer A. Prior to use, the RNA was heated to 95 °C for 1 min and snap-cooled in ice water to promote hairpin formation. For the gel mobility shift assay, the ΨSL2 RNA was first dephosphorylated on the 5′-end with calf alkaline phosphatase (Roche Molecular Biochemicals, IN) and then 5′-end-labeled with γ-(^{32}P) ATP (MP Biomedicals, CA) using T4 polynucleotide kinase (New England Biolabs, MA) according to the manufacturer's instructions.

The complex of ^{15}N-labeled NCp7 with ΨSL3 RNA was prepared by titrating ^{15}N-labeled NCp7 into ΨSL3 RNA in NMR buffer B (20 mM sodium phosphate buffer pH 7.0, 25 mM NaCl) in 90% H_2O/10% D_2O. Complex formation was monitored by 1D ^{15}N-decoupled watergate[33] and 2D ^{1}H−^{15}N HSQC.[34] Once a 1:1 complex was prepared, the sample was flash frozen and lyophilized. The sample was then resuspended to achieve a final buffer composition of 20 mM sodium phosphate pH 7.0, 100 mM NaCl in 90% H_2O/10% D_2O.

UV/Visible Spectroscopy. For UV/visible spectroscopy studies, cobalt-refolded NCp7 (150 μM) was incubated with the appropriate thioester compound or compound **3** (150 μM unless specified otherwise) at 25 °C. The UV/visible spectrum was recorded from 220 to 800 nm every 0.5 h for 3 h using a Shimadzu UV-1601 spectrophotometer equipped with PC control via the UVPC software (Shimadzu Scientific Instruments, MD). The tetrahedrally coordinated cobalt ions of NCp7 have absorption maxima at 642 and 698 nm. The absorbance at these two wavelengths was specifically monitored and compared against a control sample in which no thioester compound was added. Experiments were repeated a minimum of three times. Normalized absorbance values were calculated by subtracting the absorbance monitored by that of the control sample. The normalized absorbance at 642 and 698 nm was plotted versus time, and the initial rate of absorbance loss (0−3 h) was obtained from the slope of the linear regression analysis. In one set of experiments, compound **3** (150 μM) was incubated with acetyl CoA (Sigma-Aldrich, St. Louis, MO) (150 μM) for 1 h prior to addition of NCp7 (150 μM). Once NCp7 was added, the UV/visible spectrum was monitored as described above. The rate of absorbance loss was calculated as described above using absorbance values normalized against a control sample in which NCp7 was incubated with acetyl CoA alone.

NMR Spectroscopy. The zinc-refolded ^{15}N-labeled NCp7 (1 mM) was incubated with an equimolar concentration of thioester compound at 25 °C for 48 h in NMR buffer A and 90% H_2O/10% D_2O. The pH of the sample was checked both before and after the incubation period to ensure that any changes observed in the NMR spectra were not due to changes in pH. The sample was analyzed on Varian Unity INOVA 500 or 600 MHz spectrometers equipped with HCN triple resonance probes with actively shielded z-gradients. Three experiments were recorded at various times: a 1D ^{15}N-decoupled watergate,[33] a 1D difference water-sLED,[35] and a 2D ^{1}H−^{15}N HSQC.[34] 1D difference water-sLED experiments[35] were recorded to detect the resonances of the faster diffusing component(s) of the sample, the free thioester compounds and their derivatives produced by incubation with NCp7. In this 1D difference experiment, two water-sLED spectra, A and B, were recorded. The only parameter that differs between these two spectra is the strength of the encoding and decoding pulse-field gradient pulses, 7 G/cm in spectrum A and 14 G/cm in spectrum B. The duration of these pulses and the time delay between these pulses was set to 0.007 and 1.7 s, respectively. The 1D difference water-sLED spectrum was obtained by Fourier transformation of [FID(A) − alphaFID(B)], where the value of alpha was determined empirically to filter out the resonances of the slowly diffusing component of the sample, the NCp7 protein. The 2D ^{1}H−^{15}N HSQC spectra were processed with NMRPipe[36] and analyzed with PiPP.[37] The measured signal intensities of the HSQC signals were plotted versus time (from 0 to 48 h), and the initial rate of signal intensity loss from 0 to 24 h was obtained by linear regression.

^{1}H, ^{15}N, and ^{13}C backbone assignments for NCp7 in 90% H_2O/10% D_2O at pH 6.0, 25 °C were obtained with a ^{13}C/^{15}N-labeled sample from the following experiments: 2D ^{1}H−^{15}N HSQC,[34] 3D HNCO,[38] 3D HNCACB,[39−41] and 3D (HB)CBCA(CO)-NNH.[39,41] ^{1}H and ^{15}N chemical shift assignments for NCp7 complexed with ΨSL3 RNA were generously provided by Dr. M. F. Summers (University of Maryland, Baltimore County). ^{1}H chemical shift assignments for compound **1** were obtained from the following experiments: 1D ^{1}H watergate,[33] 2D ^{1}H−^{1}H DQF−COSY and 2D ^{1}H−^{1}H NOESY. Partial ^{1}H chemical shift assignments for compound **2** were obtained by comparison of the 1D ^{1}H watergate spectrum of the thioester compound with that of compound **1**.

Mass Spectrometry. A 1 mM sample of zinc-refolded NCp7 was incubated for 48 h with 1 mM compound **1** or **2** at 25 °C. Aliquots were taken immediately following thioester addition and then after 1, 3, 5, 7, 9, 24, and 48 h. The samples were promptly flash frozen in liquid nitrogen and lyophilized to stop the thioester activity. Lyophilized samples were resuspended in 0.05% TFA and separated on a C-18 reverse phase column using a linear gradient (5−50%) of 90% acetonitrile containing 0.04% TFA. The lyophilized NCp7 was redissolved in 50% methanol and 1% acetic acid. Samples were introduced into an LCQ Classic ion trap mass spectrometer (Thermo Electron Corp) fitted with an electrospray ionization (ESI) source. Under acidic conditions, ESI produces multiple charge states of the NCp7 protein within the range 0 to 2000 *m/z*. Spectra were deconvoluted over the range of 5000 to 7500 Da using Xcalibur Biomass software (Thermo Electron Corp). Peak areas were calculated assuming Gaussian peak shape.

For ESI-MS studies, the lyophilized NCp7 was redissolved in a minimal volume of 20 mM Tris pH 7.8, 5 mM $CaCl_2$ and 2 mM DTT. Clostripain (Promega) was added at a ratio of 1:20 with NCp7 and incubated for 3 h at 37 °C. Mass spectrometric data for the clostripain peptides were obtained from collision induced dissociation (CID) spectra.[28]

For the identification of the site of NCp7 modification, 250 μM zinc-refolded chemically synthesized NCp7 was incubated with equimolar concentration of compound **4** in 20 mM phosphate buffer pH 7.0 in a total volume of 250 μL for 3 h at 25 °C (chemical synthesis was performed as described[28]). The samples were purified on a C-18 reverse phase (Vydac) HPLC column using a gradient of 5−30% acetonitrile in 0.05% aqueous trifluoroacetic acid (TFA), and each peak was collected

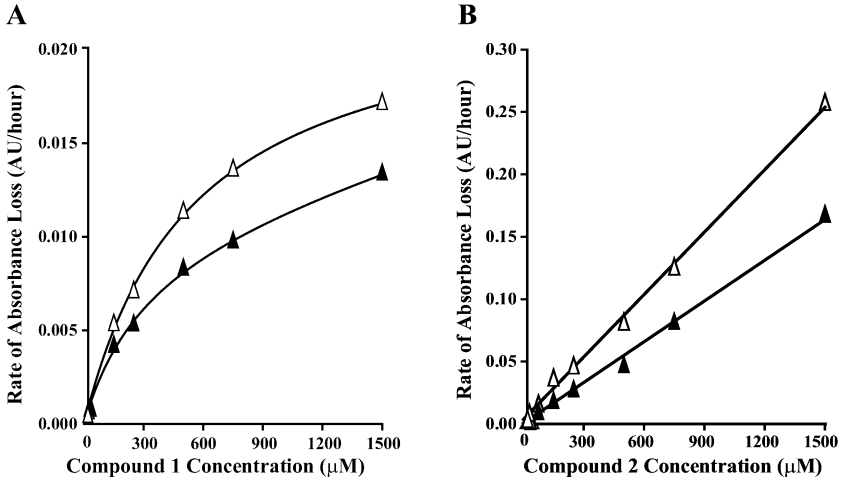

Figure 3. Rate of absorbance loss from the UV/visible spectra recorded of cobalt- refolded NCp7 incubated with either compound **1** (A) or compound **2** (B). In all experiments, the cobalt-refolded NCp7 was kept at a constant concentration (150 μM), whereas the thioester concentration was varied from 0.15 to 1500 μM. In each figure, △ is the rate of absorbance loss at 642 nm and ▲ is the rate of absorbance loss at 698 nm. Rates were calculated as described in Materials and Methods.

separately. These fractions were analyzed by MALDI-TOF and lyophilized. The lyophilized acetylated fraction was incubated for 1 h with *N*-ethylmaleimide (NEM) at a peptide:NEM molar ratio of 1:150 in 20 mM phosphate buffer pH 7.0, 0.5 mM EDTA at 30 °C. The modified peptide was then separated by HPLC separation, followed by MALDI-TOF analysis. These fractions were next subjected to clostripain digestion, HPLC separation, and MALDI-TOF analysis. The fractions of interest were further treated with chymotrypsin at 30 °C for 1 h in 10 mM Tris pH 7.0, 1.5 mM $CaCl_2$, 1.5 mM EDTA. HPLC separation, MALDI-TOF analysis, and finally ESI-MS/MS were performed.

Gel Mobility Shift Assay. A 1 μM sample of zinc-refolded NCp7 was incubated with 5.0 μM of either compound **1** or **2** in 50 mM Tris pH 7.5, 10% glycerol at 25 °C for 0 min, 5 h, and 24 h. After each incubation period, a 5 μL aliquot was removed and incubated with an equal volume of 5′-^{32}P-labeled ΨSL2 RNA (2.5 nM) in 50 mM Tris pH 7.5, 10% glycerol, 25 μg/mL yeast tRNA, 200 mM KCl, and 40 mM $MgCl_2$ for 30 min at 25 °C. The binding reactions were analyzed on an 8% native polyacrylamide gel in 50 mM Tris-Borate pH 8.0, and 1 mM EDTA at 200 V and 4 °C. The 5′-^{32}P-labeled ΨSL2 RNA was detected using a Storm PhosphorImager (Amersham Biosciences, NJ).

Results

Thioester Compounds 1 and 2 Cause Loss of Metal Coordination by NCp7. The ability of compounds **1** and **2** (Figure 2) to eject metal from NCp7 was initially studied by UV/visible spectroscopy. In these experiments, apo-NCp7 was refolded with the spectroscopically active metal Co^{2+} rather than the spectroscopically inactive metal Zn^{2+}. Whereas zinc has a full outer shell, cobalt does not, allowing d−d transitions that absorb in the UV/visible region of the spectrum. The cobalt-refolded NCp7 was incubated with various concentrations of each thioester compound, and the cobalt ejection was monitored. NCp7 refolded with Co^{2+} has two absorption maxima in the visible range: one at 642 nm and one at 698 nm.[42] These two absorption maxima correlate with the two different d−d transitions characteristic of tetrahedral geometry in which the ligands are three cysteines and one histidine.[43] If cobalt is ejected from NCp7 in the presence of the thioester compounds, a reduction in absorbance at 642 and 698 nm will be observed. Because both cobalt-bound zinc-binding domains absorb at these wavelengths, it was not possible using this assay to determine if the metal is ejected from both metal-binding domains or selectively from a single one.

Table 1. Rate of UV/Visible Absorbance Loss at 642 nm Due to Interaction of Various Compounds With NCp7

compound	rate (mAU/h)
1	3.9 ± 1.3
2	36 ± 3.7
3	0.4 ± 0.1
4	29.6 ± 2.0
3 + acetyl CoA	5.1 ± 1.6

Both compounds **1** and **2** cause a loss of absorbance over time at 642 and 698 nm (Figure 3), indicating that cobalt is no longer tetrahedrally coordinated by NCp7, and most likely ejected. On the basis of these results, it is clear that both thioester compounds are capable of ejecting metal from NCp7, and this process does not require activation with silver ions. Reduced absorption at 642 and 698 nm was tabulated at various times and used to calculate the initial rate of cobalt ejection from the zinc-binding domains. The absorbance at these two wavelengths decreased linearly over the period studied (0−3 h). The total absorbance loss was never more than 20% of the original absorbance. The rate of absorbance loss can therefore be considered as initial rates of metal ejection. These rates of absorbance loss were also calculated at various concentrations of compounds **1** and **2** (Figure 3). The observed rate of absorbance loss increases linearly with thioester concentration from 0.15 μM to 1500 μM for compound **2** and from 0.15 μM to 500 μM for compound **1** (Figure 3). Compound **1** and compound **2** show very different reaction rates from one another. At equimolar concentrations with NCp7 (150 μM), compound **2** reacts nine times more rapidly with cobalt-bound NCp7 than does compound **1** (Figure 3 and Table 1).

Thioester Compounds Show Specificity in the Reactivity with the Zinc-Binding Domains of NCp7. From the UV/visible spectroscopy experiments, it is evident that both compound **1** and compound **2** eject cobalt from NCp7. However, as previously mentioned, whether one or both zinc-binding domains are being affected cannot be determined using this experimental

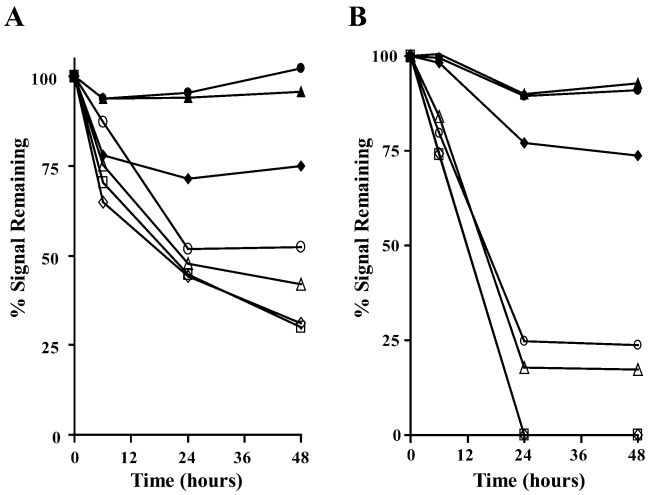

Figure 4. Change in 2D $^{1}H-^{15}N$ HSQC signal intensity of NCp7 zinc-coordinating residues after addition of compound **1** (A) and compound **2** (B). In each plot, ◆ is Cys_{15}, ▲ is His_{23}, ● is Cys_{28}, ◇ is Cys_{36}, □ is Cys_{39}, △ is His_{44}, ○ is Cys_{49}. The signal intensity of the ZD1 zinc-coordinating residue Cys_{18} was not monitored because its chemical shift changes during the course of the incubation with thioester compounds **1** and **2**.

technique. Thus, NMR spectroscopy was used to gain a more detailed understanding of the mechanism of metal ejection. Equimolar amounts of zinc-refolded ^{15}N-labeled NCp7 and compound **1** were mixed, and 2D $^{1}H-^{15}N$ HSQC experiments were used to observe changes in the $^{1}H-^{15}N$ correlations of the ^{15}N-labeled NCp7 over a period of 48 h. Immediately after the addition of compound **1**, there was no change in the 2D $^{1}H-^{15}N$ HSQC spectrum of NCp7 (Figure 1A in Supporting Information). This demonstrates that NCp7 did not undergo a structural change when the thioester compound was added and that no stable interaction was formed between NCp7 and compound **1**. Indeed, chemical shift changes would have been expected if NCp7 were making a stable complex with the thioester compound. The primary change observed in the 2D $^{1}H-^{15}N$ HSQC spectrum over 48 h was a loss of signal intensity for several signals (Figure 1B in Supporting Information). Loss of NCp7 signal intensity in the 2D $^{1}H-^{15}N$ HSQC spectrum was significantly greater for residues in ZD2 than for residues in ZD1. After 24 h, Cys_{36} and Cys_{39} in ZD2 retained only 40% of their original signal intensity, whereas Cys_{15} and Cys_{28} in ZD1 retained 85% of their original signal intensity (Figure 4A). When the change in signal intensity of zinc-binding residues is plotted over time, the distinction between the two zinc-binding domains is clear (Figure 4A). The $^{1}H-^{15}N$ correlations of the ZD1 zinc-coordinating residues Cys_{15}, His_{23}, and Cys_{28} show only a small overall change in signal intensity over 48 h. However, the $^{1}H-^{15}N$ correlations of the ZD2 zinc-coordinating residues Cys_{36}, Cys_{39}, His_{44}, and Cys_{49} lose at least 50% of their signal intensity. The initial rate of signal intensity loss is on average 10 times faster for residues in ZD2 than for residues in ZD1 (Table 2). The disparity in the signal intensity changes between residues in ZD1 and residues in ZD2 clearly indicates that compound **1** preferentially reacts with ZD2 over ZD1.

The signals for a few residues in ZD1 did undergo amide chemical shift changes during the incubation with compound **1** (Figure 1B in Supporting Information). We observed that both the amide ^{1}H and ^{15}N chemical shifts changed by at least 0.2 ppm for Phe_{16}, Asn_{17}, Cys_{18}, and Ala_{25} in ZD1. Similar amide chemical shift changes have been reported for Asn_{17} for NCp7 with no zinc coordinated in ZD2.[23] Over the course of the assay, the intensity in these shifted signals increased. Interestingly, we observed that the rate of chemical shift change for these signals is similar to the rate of disappearance of signals in ZD2 (data not shown). It therefore appears that unfolding ZD2 by compound **1** correlates with small chemical shift changes in residues located in ZD1. The fact that residues in ZD1 are affected by unfolding of ZD2 is not surprising; a dynamic interaction between the two zinc-binding domains has been reported by others.[14,28,44]

Table 2. Average Rate of Loss of 2D $^{1}H-^{15}N$ HSQC Signal Intensity for Zinc-Coordinating Residues in NCp7

		rate (% intensity/h)	
thioester	NCp7 state	ZD1	ZD2
1	free	0.11 ± 0.18	1.20 ± 0.10
	complex	0.27 ± 0.22	0.34 ± 0.21
2	free	0.33 ± 0.18	3.70 ± 0.40
	complex	0.01 ± 0.05	0.21 ± 0.01
3	free	0.08 ± 0.01	0.45 ± 0.04

The NMR results obtained when compound **2** was incubated with NCp7 were similar to those obtained with compound **1**. The 2D $^{1}H-^{15}N$ HSQC spectrum does not change much immediately following compound **2** addition (Figure 2A in Supporting Information), indicating that the NCp7 structure remains intact. Over time, most amide signals lose intensity rather than undergo chemical shift changes (Figure 2B in Supporting Information). After 24 h, signals that correspond to residues in ZD2 lost more intensity than those from ZD1 (Figure 4B). Signals for Cys_{36} and Cys_{39} disappeared within 24 h of addition of compound **2**. His_{44} and Cys_{49} signals retained less than 25% of their original intensity by 24 h. In contrast, ZD1 residues Cys_{15}, His_{23}, and Cys_{28} retained at least 80% of their original intensity even after 48 h of incubation. Like compound **1**, compound **2** shows a clear specificity for ZD2. However, the reaction of compound **2** with ZD2 is three times faster than that of compound **1** (Table 2). This general trend agrees with that observed in the UV/visible experiments with cobalt-refolded NCp7. The overall rate of change was, however, faster with cobalt-refolded NCp7 than with zinc-refolded NCp7. This difference likely reflects the different affinities of NCp7 for the two metals. As zinc is coordinated by NCp7 with a 10^3 lower K_D than cobalt,[45] it is expected that the ejection of zinc would take longer than that of cobalt. The specificity toward ZD2 is also more clearly observed with compound **2** than compound **1** (Figure 4). The more pronounced specificity of compound **2** is likely a result of the higher activity of this thioester compared to compound **1**.

Disappearance of Free Thioester Compounds upon Incubation with NCp7. The 1D difference water-sLED spectrum was used to monitor changes in compound **1** and compound **2** when they were mixed with equimolar concentrations of ^{15}N-labeled NCp7. The difference water-sLED spectrum collected immediately after addition of compound **1** to NCp7 (Figure 5A) is identical to the spectrum of the free thioester compound

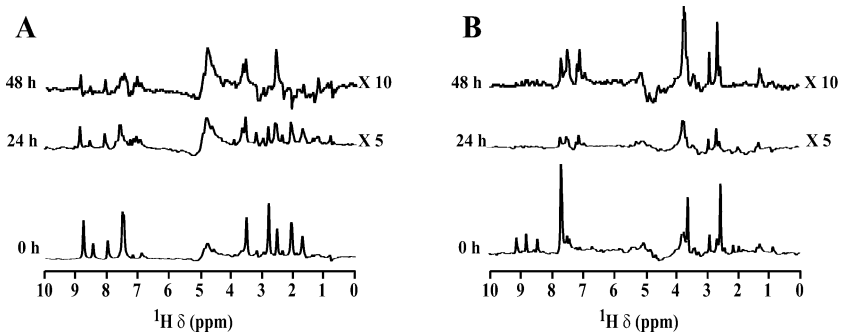

Figure 5. 1D difference water-sLED spectra of NCp7 incubated with compound **1** (A) or compound **2** (B). In both A and B, spectra are shown after 0, 24, and 48 h.

(data not shown). Over time, all compound **1** signals decreased in intensity, and by 48 h the signals are generally indistinguishable from subtraction artifacts (Figure 5A). To ensure that the decrease in signal intensity in the difference water-sLED spectrum was not due to the natural instability of compound **1**, we incubated the thioester compound in NMR buffer over 48 h. After 48 h, there was no change in the 1D ^{1}H spectrum of compound **1** (data not shown). This indicates that the loss of signal intensity seen in the difference water-sLED spectra is due to either the interaction of compound **1** with NCp7 or chemical reactivity due to the presence of NCp7. In the case of compound **2**, we also did not see any change immediately after addition of the thioester compound to NCp7 (data not shown). Over time, the difference water-sLED spectra show that some peaks from compound **2** disappear, whereas others decrease in intensity, but never completely disappear (Figure 5B). After only 6 h, three peaks between 8.1 and 9.4 ppm have completely disappeared. These peaks correspond to protons in the nicotinoyl moiety unique to compound **2** (Figure 2). Peaks from the 2-mercaptobenzamide portion of compound **2** decrease in intensity, but do not disappear completely. This suggests that the nicotinoyl moiety is rapidly binding and/or reacting with NCp7, whereas the 2-mercaptobenzamide moiety undergoes a slower uncharacterized secondary binding event and/or reaction.

Thioester Compounds Covalently Modify NCp7. From the UV/visible and NMR spectroscopy experiments, it was shown that compounds **1** and **2** specifically react with ZD2 of NCp7, eject coordinated metal from the protein, and cause unfolding of ZD2. Based on these results, we hypothesized that the thioester compounds are modifying cysteine residues in ZD2, leading to zinc ejection. To test this hypothesis, we used mass spectrometry to identify any modifications to NCp7 following addition of compound **1**. Equimolar amounts of zinc-refolded NCp7 and each thioester compound were incubated for up to 48 h. The ESI-MS spectrum of an aliquot removed 1 h after the addition of compound **1** shows an envelope of peaks corresponding to multiple charge states of unmodified NCp7 with an additional, lower-intensity envelope of higher-mass peaks (Figure 3A in Supporting Information). The deconvoluted mass spectrum (Figure 3B in Supporting Information) contained two peaks, one at 6425 ± 1 Da, corresponding to intact NCp7, and one at 6587 ± 1 Da, corresponding to a modified form. The net difference between the two masses results from the loss of a proton and addition of a modification with a mass of 163 Da, consistent with the pyridinioylalkanoyl moiety of compound **1**. During the initial 7 h of incubation, the amount of singly modified species increases while the unmodified form decreases (Figure 6). The deconvoluted mass spectra of aliquots taken at later times contain peaks of higher mass that are consistent with NCp7 being modified with two or three similar adducts.

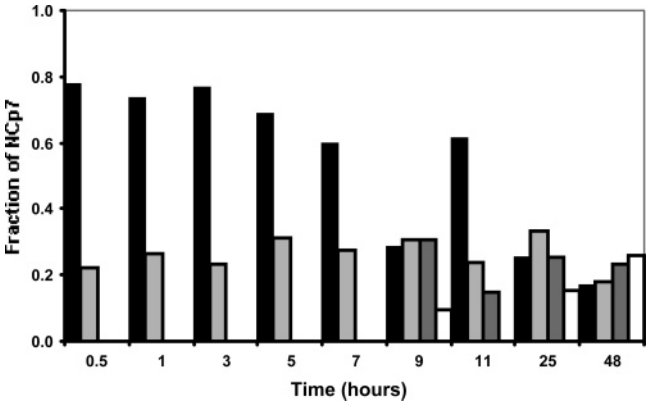

Figure 6. Mass spectrometry analysis of NCp7 modifications by compound **1** at various times. The relative amount of NCp7 with no modification is shown in black, one modification in light gray, two modifications in dark gray, or three modifications in white.

Reactivity of NCp7 with the Free Thiol. The mass spectral analysis raises a new question: What happens to the thiol group if only the acyl moiety is found attached to NCp7? The 1D difference water-sLED spectra show that all of the protons from compound **1** eventually disappear (Figure 5A). The difference water-sLED spectra from the experiments with compound **2** also show large loss of signal intensity from protons in the thiol moiety (Figure 5B). Thus, the NMR experiments suggest that something does happen to the thiol moiety.

To determine the effect of the thiol group on NCp7, we studied the interaction of NCp7 with the free thiol formed after thioester cleavage (compound **3**, Figure 2). The activity of compound **3** was analyzed first by UV/visible spectroscopy experiments with cobalt-refolded NCp7 in a sealed cuvette with degassed buffer to prevent oxidation (data not shown). Over a period of 3 h, there was no significant change in absorbance at 642 nm compared to a control sample (Table 1). Thus, in this assay, compound **3** was at least 9.8 times slower than compound **1** and 90 times slower than compound **2** at ejecting the bound cobalt from NCp7.

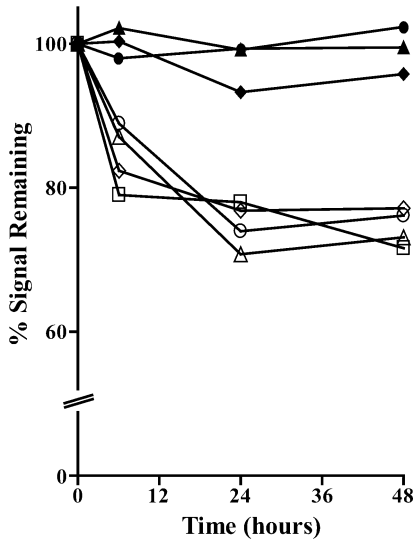

Figure 7. Change in 2D $^{1}H-^{15}N$ HSQC signal intensity of zinc-coordinating residues after compound **3** addition to NCp7. In the plot, ◆ is Cys_{15}, ▲ is His_{23}, ● is Cys_{28}, ◇ is Cys_{36}, □ is Cys_{39}, △ is His_{44}, ○ is Cys_{49}.

NMR experiments were next performed with compound **3** using degassed NMR buffer in a sealed NMR tube. The difference water-sLED spectra for compound **3** did not change over the entire incubation period (data not shown). There was a small loss of NCp7 signal intensity in the 2D $^{1}H-^{15}N$ HSQC spectra for residues in ZD2 when incubated with compound **3** (Figure 7, Table 2). After 48 h, the signals for zinc-coordinating residues in ZD2 retained 71−78% of their original intensity, whereas the corresponding signals in ZD1 retained 85−100% of their original intensity (Figure 7). The average rate of signal intensity loss in ZD2 due to compound **3** is 2.5 times lower than that seen with compound **1** (Table 2). Like the active thioester compounds, the activity of compound **3** seems to be specific for ZD2, but its overall activity is very low.

In the cellular environment, there are many potential reactions that a free thiol, such as compound **3**, can undergo. For example, the thiol can react with glutathione or be acylated by acyl CoA derivatives. To test the potential reactivity of one reaction product of compound **3**, we used UV/visible spectroscopy to analyze the effect of compound **3** incubated with acetyl CoA and the effect of the acetylated form of the thiol (compound **4**). When we first incubated compound **3** with acetyl CoA and then with cobalt-refolded NCp7, we observed a loss of cobalt absorbance (Table 1). We also incubated cobalt-refolded NCp7 with preformed acetylated-compound **3**, compound **4** (Figure 2). With compound **4**, we also observed a loss of cobalt absorbance (Table 1). The rate of absorbance loss for compound **4** was similar to that observed for compound **2**, demonstrating high reactivity of this compound toward cobalt-refolded NCp7. However, the lower rate observed for thiol mixed with acetyl CoA suggests that the transfer of acetyl group from CoA to thiol may have been incomplete under the conditions of the experiment.

We further characterized the interaction of compound **4** with NCp7 by NMR spectroscopy. As with compounds **1** and **2**, we incubated equimolar concentrations of compound **4** with NCp7 and monitored changes in NCp7 by 2D $^{1}H-^{15}N$ HSQC spectra. There was no change in the 2D HSQC spectrum of NCp7 immediately following the addition of compound **4**, indicating that there was no conformational change in NCp7 upon mixing with the thioester compound (data not shown). After 48 h of incubation with compound **4**, we observed loss of signal intensity for residues of ZD2 (data not shown). These changes are the same as those seen upon NCp7 incubation with compounds **1** and **2**. This indicates that compound **4** interacts with NCp7 in a similar manner as the other thioester compounds that we have analyzed. These results suggest that the thiols freed by reaction of the thioester compounds with NCp7, or by enzyme-promoted hydrolysis, could be re-acylated intracellularly by acyl CoA derivatives. The newly formed thioester would then be available to interact with additional NCp7 molecules.

Thioester Reaction with NCp7 Occurs First with Cys_{39}. Mass spectrometry was next used to determine which residues of NCp7 are the first to interact with the thioester compounds. Following incubation of compound **4** with NCp7, samples were subjected to tandem mass spectral analysis of constituent peptides (see methods) to identify residues of NCp7 that had reacted. This analysis revealed that the first modification of NCp7 occurred primarily on Cys_{39}, with a minor population with modification to Cys_{49} (data not shown). As NMR spectroscopy analysis showed that compound **4** interacts with NCp7 in a similar manner as compounds **1** and **2**, it is likely that the modification on Cys_{39} is a typical feature of thioester interaction with NCp7.

Nucleic Acid Binding Both Inhibits and Is Inhibited by Thioester Compound Interaction. Since NCp7 has nucleic acid binding activity in vivo, it is important to analyze the effect of thioester compounds not just on the free protein, but also on NCp7 complexed with nucleic acid. We made a complex between NCp7 and the third stem-loop (ΨSL3) from the Ψ-region at the 5′-end of the HIV-1 viral RNA (Figure 1B). NCp7 has been shown to bind ΨSL3 with a K_d = 28 nM,[46] and the three-dimensional structure of the NCp7/ΨSL3 RNA complex has been determined by NMR spectroscopy.[47] We first determined that compound **1** did not have an effect on the free ΨSL3 RNA (data not shown). Then, the zinc-refolded NCp7/ΨSL3 complex was incubated with an equimolar concentration of either compound **1** or compound **2**. The effect of the thioester compound with the complex was analyzed using NMR spectroscopy over a period of 48 h.

The difference water-sLED spectrum recorded immediately after addition of compound **1** to the complex showed no changes in the thioester compound (data not shown). Likewise, the 2D $^{1}H-^{15}N$ HQSC spectrum recorded immediately after compound **1** addition shows no chemical shift changes in the complexed protein. Together these two observations indicate that neither the protein/RNA complex nor compound **1** undergo any change upon mixing.

Over time, the difference water-sLED spectra show only minor changes in compound **1** (data not shown). There is a small amount (<10%) of signal intensity loss after 48 h. This result is very different from what was seen with the uncomplexed protein, where all of the compound **1** signals disappeared by 48 h. This suggests

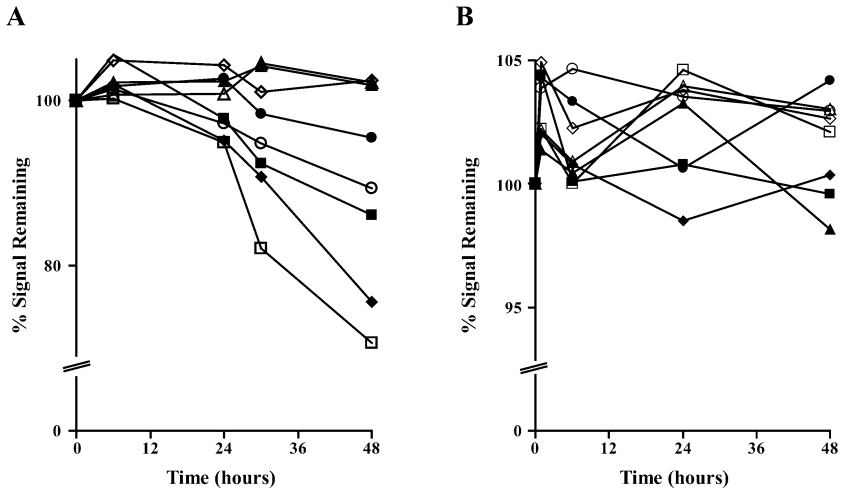

Figure 8. Change in 2D $^{1}H-^{15}N$ HSQC signal intensity of zinc-coordinating residues after addition of compound **1** (A) or compound **2** (B) to an NCp7/ΨSL3 RNA complex. In each plot ◆ is Cys_{15}, ■ is Cys_{18}, ▲ is His_{23}, ● is Cys_{28}, ◇ is Cys_{36}, □ is Cys_{39}, △ is His_{44}, ○ is Cys_{49}.

that the compound **1** does not interact with the NCp7/RNA complex, as its diffusion rate does not change over 48 h. The 2D $^{1}H-^{15}N$ HSQC spectra of complexed NCp7 also reveal only a small loss of signal intensity in both zinc-binding domains over the period of the incubation (Figure 8A, Table 2). After 48 h, the zinc-coordinating residues of both ZD1 and ZD2 had lost 10% of their signal intensity (Figure 8A). The overall reactivity of compound **1** toward ΨSL3-bound NCp7 is greatly reduced compared with the reactivity toward free NCp7. The rate of signal intensity loss of ZD2 with free NCp7 is 3.5−4 times faster than that of ΨSL3-bound NCp7 (Table 2).

The effect of compound **2** on the ΨSL3-bound NCp7 is similar to that of compound **1**. The difference water-sLED spectra recorded during the incubation with compound **2** do not change over 48 h (data not shown). There is no change in signal intensity and chemical shift. As with compound **1**, there is no evidence from the 1D difference water-sLED experiments that compound **2** interacts with NCp7 bound to ΨSL3 RNA. The 2D $^{1}H-^{15}N$ HSQC spectra also remain the same throughout the incubation. There is essentially no change in signal intensity and chemical shift for any residues in NCp7 (Figure 8B, Table 2). Thus, interaction with the HIV-1 ΨSL3 RNA protects the zinc-coordinating residues of NCp7 from reacting with these two thioester compounds.

Gel mobility shift assays were used to investigate the effect of the thioester compounds on the nucleic acid binding properties of NCp7. Zinc-refolded NCp7 was incubated with either compound **1** or compound **2** and then mixed with the second stem loop (ΨSL2) from the HIV-1 Ψ site ($K_d = 23$ nM[46]). Addition of NCp7 to ΨSL2 RNA caused a gel mobility shift of the ^{32}P-labeled RNA (Figure 9, lanes 1, 2, and 5). The presence of a gel mobility shift in samples where NCp7, ΨSL2 RNA, and thioester compounds were briefly mixed indicates that neither compound **1** nor compound **2** immediately affects the RNA binding properties of NCp7 (Figure 9, lanes 3 and 4). However, after 24 h of NCp7 and thioester incubation, NCp7 no longer caused retardation of ΨSL2 RNA in the native gel (Figure 9, lanes 6 and 7). Since the ejection of zinc from NCp7 by compound **1** or

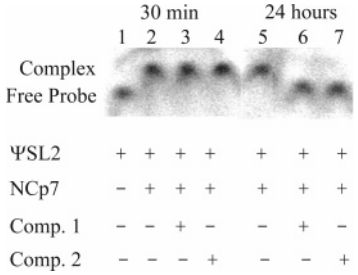

Figure 9. Gel mobility shift assay to study the effect of thioester compounds on binding of NCp7 to ΨSL2 RNA. NCp7 was incubated without (lanes 2 and 5) or with a thioester compound [compound **1** (lanes 3 and 6) or compound **2** (lanes 4 and 7)] for 30 s or 24 h. Except for the control lane 1, ^{32}P-labeled ΨSL2 RNA was then added and incubated for 30 min at 25 °C before being run on the 8% native gel.

compound **2** causes a loss of the structural integrity of ZD2, NCp7 likely loses its affinity for ΨSL2 RNA after reaction with the thioester compounds.

Discussion

Our studies demonstrate that the new thioesters (compounds **1** and **2**) are able to eject coordinated metals from the zinc-binding domains of NCp7. The new compounds appear to be more reactive than earlier thioesters, as they did not require the addition of silver ions to activate metal ejection from NCp7. Like the DIBA compounds and earlier thioester compounds, both compound **1** and compound **2** showed specificity for ZD2 of NCp7.[23,25,26,28,48,49] From NMR experiments, we observed that compound **2** completely unfolded ZD2, whereas ZD1 was essentially unaffected. Clearly, even though the two zinc-binding domains of NCp7 are structurally alike and contain similar amino acid composition,[50] there is a large variation in their reactivity. The surrounding residues in each zinc-binding domain must make a significant contribution to the overall reactivity and/or accessibility of each zinc-binding domain.

With the combined information from the UV/visible spectroscopy, NMR spectroscopy, and mass spectrometry, we can propose a reaction mechanism for the interaction of the thioester compounds **1** and **2** with NCp7 (Figure 10). The sulfhydryl group of Cys_{39} makes

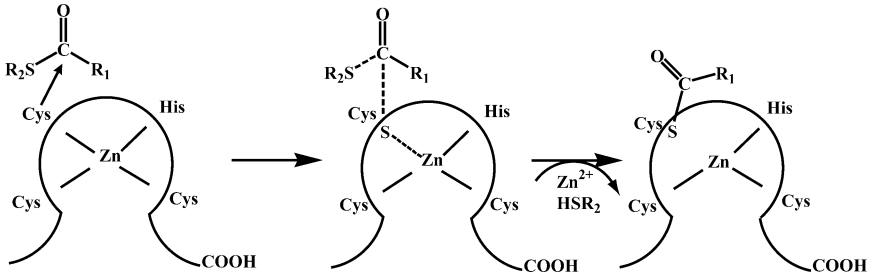

Figure 10. Schematic of the proposed thioester reaction mechanism. Cys_{39} in ZD2 makes a nucleophilic attack on the carbonyl carbon of the thioester compound. This results in loss of zinc coordination by Cys_{39} and destruction of the thioester bond of the thioester compound. A new thioester linkage is formed between the R_1 moiety and Cys_{39}. Once zinc coordination is destabilized, other cysteine residues in the zinc-binding domain become more susceptible to thioester reaction. Eventually, the zinc is ejected from the zinc-binding domain, which leads to loss of structure.

a nucleophilic attack on the carbonyl carbon of the thioester compound, leading to a covalent modification of the sulfhydryl group (acyl transfer). This results in a covalently modified cysteine in NCp7 and release of a free thiol from the thioester (compound **3**). In this process, a new thioester bond is formed between the cysteine sulfur in NCp7 and the pyridinioalkanoyl moiety of compound **1** or the nicotinoyl moiety of compound **2**. Loss of zinc coordination by Cys_{39} makes the other cysteine residues in the zinc-binding domain more susceptible to subsequent reaction with the thioester compound or the free thiol. At some point, zinc is ejected from the zinc-binding domain causing a loss of the ZD2 fold. Once ZD2 is unfolded, ZD1 is likely destabilized and also undergoes a structural change. As we have shown, NCp7 is then no longer able to bind to nucleic acids. The loss of structure prevents the protein from fulfilling its numerous functions associated with its ability to specifically bind RNA.

In all of our experiments, compound **2** was more reactive than compound **1**. In the UV/visible spectroscopy experiments, the rate of absorbance loss for compound **2** was ~10 times faster than that calculated for compound **1** (Figure 3, Table 1). Likewise, compound **2** caused 3 times faster loss of signal intensity than compound **1** for signals of residues in ZD2 in the 2D $^1H-^{15}N$ HSQC spectra. Interestingly, compound **4** ejected metal from cobalt-refolded NCp7 at approximately the same rate as compound **2** in the UV/visible spectroscopy experiments. Compounds **1**, **2**, and **4** all contain the same 2-mercaptobenzamide thiol group (Figure 2). Thus, the variation in the activity of the three thioester compounds must be due to inherent differences between the pyridinioalkanoyl moiety of compound **1**, the nicotinoyl moiety of compound **2**, and the acetyl moiety of compound **4**. The acetyl and nicotinoyl groups have smaller electron donating effects on the carbonyl carbon of the thioester, which could make the nucleophilic reaction with Cys_{39} proceed faster with compound **2** or **4** than with compound **1** (Table 1).

A similar study to that reported here was conducted with DIBA compounds, in which it was found that the compound reacted primarily with ZD2.[23] The proposed reaction mechanism of the DIBA compounds in vitro is dissimilar to the mechanism we propose for the thioesters: whereas thioester compounds transfer their acyl group initially to Cys_{39}, there is a thiol−disulfide interchange between the DIBA compound and NCp7 at Cys_{36} and Cys_{49}.[23] Modifications by both the thioester and DIBA compounds lead to loss of zinc coordination. Additionally, the study of NCp7 reactivity with NEM found Cys_{49} to be the first site of reaction with this alkylating agent.[49] In the 2D $^1H-^{15}N$ HSQC experiments with compounds **1** and **2**, Cys_{49} showed the lowest loss of signal intensity compared with the other zinc-coordinating residues in ZD2. After 48 h of incubation with compound **2**, the signal for Cys_{49} retained 25% of its original signal intensity, whereas the signal for Cys_{39} had completely disappeared after by 24 h. Our experiments show that Cys_{49} is not affected structurally as much as Cys_{39} by the interaction with the thioester compounds. The different sites of the first reaction between the DIBA compound and the thioester compounds studied here could reflect a distinction in the binding site of the two types of compounds. When various electrophiles were docked to NCp7, it was observed that the most productive docking occurred in a pocket adjacent to Cys_{39} and Cys_{49}.[51] The DIBA compounds may interact in an orientation with easier access to Cys_{49} and the thioester compounds may more readily approach Cys_{39}. However, stable complexes between the thioester compounds and NCp7 could not be demonstrated by NMR spectroscopy.

The functions of NCp7 in the HIV-1 lifecycle revolve around the ability of the protein to bind nucleic acids. Thus, it was important to study the effect of the thioester compounds not only on the free protein, but also on RNA-bound NCp7. We showed that NCp7 is resistant to reaction with the thioester compounds when complexed to RNA. In the bound state, the zinc-coordinating residues are not solvent-accessible, and the RNA is able to protect the protein.[47,52] Thus, NCp7 is mostly susceptible to reactions with the thioester compounds when it is not bound to RNA. Once NCp7 has reacted with the thioester compounds, however, it loses its structure and is no longer able to bind RNA. Throughout the HIV-1 lifecycle, NCp7 binds to several different nucleic acids: for example, the $tRNA_3^{Lys}$ primer, the reverse transcribed cDNA, and the Ψ-site RNA. As these different nucleic acids show a large variation in sequence, secondary structure, and NCp7 binding affinity, there is likely also a range of susceptibilities of these NCp7/nucleic acid complexes from reaction with the thioester compounds. Additionally, it is unlikely that the conformation of NCp7 in the complex with each of these nucleic acids is exactly the same. The solution structure of NCp7 bound to ΨSL2 RNA is different from the solution structure of NCp7 bound to ΨSL3 RNA even though both RNAs form a stem-loop structure and have similar loop sequences.[47,52]

A previous study with *N*-ethylmaleimide (NEM) showed a range of reactivity when NCp7 was complexed with short DNA molecules of different sequences.[49] Thus, it is possible that when bound to different nucleic acid sequences, NCp7 will be differentially susceptible to reaction with the thioester compounds.

We propose that compound **3** is acylated, possibly by acyl CoA's, in vivo, producing new thioester compounds. This means that the thiol group produced upon cleavage of the thioester bond could be re-acylated and available for a second reaction with NCp7. The ability of the reaction product to undergo subsequent reactions in vivo appears to make the thioester compounds unique among zinc-ejecting compounds designed to target NCp7. For example, ADA is converted into biurea in vivo, which has no antiviral effect.[53] Interestingly, in aqueous conditions, many disulfide compounds rapidly cyclize to form a somewhat less reactive benzisothiazolone derivative and an aromatic thiol compound.[23,54−56] The aromatic thiol groups released from the DIBA compounds by glutathione reduction may behave like compound **3**, as they do not function as zinc ejectors in vitro.[55] However, it is conceivable that the DIBA-released thiols are acylated in vivo by acyl CoA to form an active thioester as we are predicting for compound **3**. Thus, the antiviral activity associated with the DIBA compounds might be due in part to their ability to form reactive thioester compounds following reduction.

The experiments shown here demonstrate that the thioester compounds **1** and **2** are able to eject coordinated zinc from NCp7 through covalent modification of Cys_{39}. The covalent modification of Cys_{39} following reaction with compounds **1** and **2** leads to structural changes that prevent NCp7 from binding to nucleic acids. In addition to modifying Cys_{39}, the reaction of compounds **1** and **2** with NCp7 results in the release of the 2-mercaptobenzoyl-β-alanamide, compound **3**. Although compound **3** itself has very little intrinsic reactivity toward NCp7, we have demonstrated that this thiol could be acylated in vitro by acetyl CoA to form a new thioester, compound **4**, which is capable of ejecting zinc from NCp7 by acylating Cys_{39}. These results suggest that the thiol formed from reaction of the thioester compounds **1** and **2** with NCp7 could be acylated in vivo by acetyl CoA or other acyl transfer agents to form a new thioester, which is able to undergo a second reaction with NCp7. This may explain the in vivo reactivity of these thioester compounds, which have the potential to be reactivated.

One feature of the thioester compounds that may be important for antiviral activity is the stability of these compounds, which is much higher in general than that of the DIBA compounds. In a recent study, the antiviral activity and the stability of a number of thioester compounds were evaluated.[31] This study demonstrated that hydrolytic cleavage of the thioester bond in human serum varied considerably depending on the structure of the *S*-acyl group.[31] For example, compound **1** [$t_{1/2}$ = 156 min (unpublished data)] is more stable than compound **2** ($t_{1/2}$ = 49 min[31]) and compound **4** [$t_{1/2}$ = 19 min (unpublished data)] in 10% human serum. The higher stability of compound **1** does not correlate with a higher in vitro reactivity for this compound, since we have shown here that compounds **2** and **4** reacted faster than compound **1** with NCp7. Furthermore, thorough analysis of the hundreds of compounds tested failed to establish a correlation between hydrolytic stability and antiviral potency.[31] One possible explanation is that the free thiols produced by hydrolytic degradation may be converted in vivo into other thioester compounds at different rates and, as a result, possess considerably different levels of antiviral activities. The same process could explain the antiviral activity of DIBA compounds, which can be reduced in solution to produce free thiols. Through these studies, we have gained a more detailed understanding of the mechanism of action of the thioester compounds, which is important for future design of compounds that target NCp7. Interestingly, our NMR results clearly demonstrate that neither the 2-mercaptobenzoyl-β-alanamide nor the *S*-acyl moieties have intrinsic binding activity toward NCp7. These results suggest that it might be possible to design thioesters with improved affinity and selectivity for NCp7 by altering the framework of the thioester compounds, especially the thiol component, so that they would be capable of specifically interacting with amino acid residues in NCp7 that are in proximity to Cys_{39}. One potential amino acid target is Trp_{37}, which is close in space to the reactive cysteine and is relatively well exposed to the solvent. Therefore, it might be possible to design thioester compounds that both interact with Trp_{37} and acylate Cys_{39}, and such compounds may possess enhanced specificity and affinity for NCp7 relative to the thioester compounds studied here. To understand the specificity of the thioesters compounds studied here, as well as those that will be designed in the future, it is crucial to investigate their effect on cellular zinc-binding proteins. Studies similar to the one presented here are currently underway to examine the mechanism of action of the thioester compounds with cellular proteins containing a variety of zinc-binding motifs.

Acknowledgment. We thank Dr. Venkatesha Basrur for his help with preliminary mass spectrometry data. This work was supported by American Cancer Society Grant RPG LBC-100183 (J.G.O.) and National Institutes of Health Grant RO1 GM60298-01 (to J.G.O and P.L.) L.M.M.J. is supported by a Presidential Graduate Fellowship from the University of Georgia. This project was funded in part by the Intramural AIDS Targeted Antiretroviral Program (IATAP).

Appendix

Abbreviations: ADA, azodicarbonamide; CID, collision-induced dissociation; DIBA, disulfide benzamide; DTT, dithiothreitol; ESI, electrospray ionization; HPLC, high-performance liquid chromatography; IPTG, isopropyl-β-D-thiogalactopyranoside; NCp7, nucleocapsid protein; NEM, *N*-ethylmaleimide; NOBA, 3-nitrosobenzamide; TFA, trifluoroacetic acid; water-sLED, water-suppressed longitudinal encode−decode; ZD1, amino-terminal zinc-binding domain; ZD2, carboxyl-terminal zinc-binding domain.

Supporting Information Available: Figure 1 shows superposition of 2D $^1H-^{15}N$ spectra of NCp7 free and after addition of compound **1** (at 0 and 48 h). Figure 2 shows superposition of 2D $^1H-^{15}N$ spectra of NCp7 free and after

addition of compound **2** (at 0 and 48 h). Figure 3 shows electrospray ionization and deconvoluted mass spectra of NCp7 following addition of compound **1** (at 1 h). This material is available free of charge via the Internet at http://pubs.acs.org.

References

(1) Cohen, J. The daunting challenge of keeping HIV suppressed. *Science* **1997**, *277*, 32−33.

(2) Finzi, D.; Hermankova, M.; Pierson, T.; Carruth, L. M.; Buck, C.; Chaisson, R. E.; Quinn, T. C.; Chadwick, K.; Margolick, J.; Brookmeyer, R.; Gallant, J.; Markowitz, M.; Ho, D. D.; Richman, D. D.; Siliciano, R. F. Identification of a reservoir for HIV-1 in patients on highly active antiretroviral therapy. *Science* **1997**, *278*, 1295−1300.

(3) Wong, J. K.; Hezareh, M.; Gunthard, H. F.; Havlir, D. V.; Ignacio, C. C.; Spina, C. A.; Richman, D. D. Recovery of replication-competent HIV despite prolonged suppression of plasma viremia. *Science* **1997**, *278*, 1291−1295.

(4) Tozser, J. Part III clinical insight − HIV inhibitors: problems and reality. *Ann. N.Y. Acad. Sci.* **2001**, *946*, 15.

(5) Guo, J.; Henderson, L. E.; Bess, J.; Kane, B.; Levin, J. G. Human immunodeficiency virus type 1 nucleocapsid protein promotes efficient strand transfer and specific viral DNA synthesis by inhibiting TAR-dependent self-priming from minus-strand strong-stop DNA. *J. Virol.* **1997**, *71*, 5178−5188.

(6) Negroni, M.; Buc, H. Mechanisms of retroviral recombination. *Annu. Rev. Genet.* **2001**, *35*, 275−302.

(7) Tisne, C.; Roques, B. P.; Dardel, F. Heteronuclear NMR studies of the interaction of tRNA(Lys)3 with HIV-1 nucleocapsid protein. *J. Mol. Biol.* **2001**, *306*, 443−454.

(8) Carteau, S.; Batson, S. C.; Poljak, L.; Mouscadet, J. F.; de Rocquigny, H.; Darlix, J. L.; Roques, B. P.; Kas, E.; Auclair, C. Human immunodeficiency virus type 1 nucleocapsid protein specifically stimulates Mg2+-dependent DNA integration in vitro. *J. Virol.* **1997**, *71*, 6225−6229.

(9) Carteau, S.; Gorelick, R. J.; Bushman, F. D. Coupled integration of human immunodeficiency virus type 1 cDNA ends by purified integrase in vitro: stimulation by the viral nucleocapsid protein. *J. Virol.* **1999**, *73*, 6670−6679.

(10) Meric, C.; Goff, S. P. Characterization of Moloney murine leukemia virus mutants with single-amino acid substitutions in the Cys-His box of the nucleocapsid protein. *J. Virol.* **1989**, *63*, 1558−1568.

(11) Darlix, J. L.; Gabus, C.; Nugeyre, M. T.; Clavel, F.; Barre-Sinoussi, F. Cis elements and trans-acting factors involved in the RNA dimerization of the human immunodeficiency virus HIV-1. *J. Mol. Biol.* **1990**, *216*, 689−699.

(12) Gorelick, R. J.; Nigida, S. M., Jr.; Bess, J. W., Jr.; Arthur, L. O.; Henderson, L. E.; Rein, A. Noninfectious human immunodeficiency virus type 1 mutants deficient in genomic RNA. *J. Virol.* **1990**, *64*, 3207−3211.

(13) Omichinski, J. G., Clore, G. M., Sakaguchi, K., Appella, E., Gronenborn, A. M. Structural characterization of a 39-residue synthetic peptide containing the two zinc binding domains from the HIV-1 p7 nucleocapsid protein by CD and NMR spectroscopy. *FEBS Lett.* **1991**, *292*, 25−30.

(14) Morellet, N., Jullian, N., De Rocquigny, H., Maigret, B., Darlix, J., Roques, B. P. Determination of the structure of the nucleocapsid protein from the human immunodeficiency virus type 1 by ^{1}H NMR. *EMBO J.* **1992**, *11*, 3059−3065.

(15) South, T. L.; Summers, M. F. Zinc- and sequence-dependent binding to nucleic acids by the N-terminal zinc finger of the HIV-1 nucleocapsid protein: NMR structure of the complex with the Psi-site analog, dACGCC. *Protein Sci.* **1993**, *2*, 3−19.

(16) Dorfman, T.; Luban, J.; Goff, S. P.; Haseltine, W. A.; Gottlinger, H. G. Mapping of functionally important residues of a cysteine-histidine box in the human immunodeficiency virus type 1 nucleocapsid protein. *J. Virol.* **1993**, *67*, 6159−6169.

(17) Housset, V.; De Rocquigny, H.; Roques, B. P.; Darlix, J. L. Basic amino acids flanking the zinc finger of Moloney murine leukemia virus nucleocapsid protein NCp10 are critical for virus infectivity. *J. Virol.* **1993**, *67*, 2537−2545.

(18) Poon, D. T.; Wu, J.; Aldovini, A. Charged amino acid residues of human immunodeficiency virus type 1 nucleocapsid p7 protein involved in RNA packaging and infectivity. *J. Virol.* **1996**, *70*, 6607−6616.

(19) Tanchou, V.; Decimo, D.; Pechoux, C.; Lener, D.; Rogemond, V.; Berthoux, L.; Ottmann, M.; Darlix, J. L. Role of the N-terminal zinc finger of human immunodeficiency virus type 1 nucleocapsid protein in virus structure and replication. *J. Virol.* **1998**, *72*, 4442−4447.

(20) Rice, W. G.; Schaeffer, C. A.; Graham, L.; Bu, M.; McDougal, J. S.; Orloff, S. L.; Villinger, F.; Young, M.; Oroszlan, S.; Fesen, M. R.; et al. The site of antiviral action of 3-nitrosobenzamide on the infectivity process of human immunodeficiency virus in human lymphocytes. *Proc. Natl. Acad. Sci. U.S.A.* **1993**, *90*, 9721−9724.

(21) Rice, W. G.; Supko, J. G.; Malspeis, L.; Buckheit, R. W., Jr.; Clanton, D.; Bu, M.; Graham, L.; Schaeffer, C. A.; Turpin, J. A.; Domagala, J.; et al. Inhibitors of HIV nucleocapsid protein zinc fingers as candidates for the treatment of AIDS. *Science* **1995**, *270*, 1194−1197.

(22) Rice, W. G.; Turpin, J. A.; Huang, M.; Clanton, D.; Buckheit, R. W., Jr.; Covell, D. G.; Wallqvist, A.; McDonnell, N. B.; DeGuzman, R. N.; Summers, M. F.; Zalkow, L.; Bader, J. P.; Haugwitz, R. D.; Sausville, E. A. Azodicarbonamide inhibits HIV-1 replication by targeting the nucleocapsid protein. *Nat. Med.* **1997**, *3*, 341−345.

(23) Loo, J. A.; Holler, T. P.; Sanchez, J.; Gogliotti, R.; Maloney, L.; Reily, M. D. Biophysical characterization of zinc ejection from HIV nucleocapsid protein by anti-HIV 2,2′-dithiobis[benzamides] and benzisothiazolones. *J. Med. Chem.* **1996**, *39*, 4313−4320.

(24) Huang, M., Maynard, A., Turpin, J. A., Graham, L., Janini, G. M., Covell, D. G., Rice, W. G. Anti-HIV agents that selectively target retroviral nucleocapsid protein zinc fingers without affecting cellular zinc finger proteins. *J. Med. Chem.* **1998**, *41*, 1371−1381.

(25) Tummino, P. J.; Scholten, J. D.; Harvey, P. J.; Holler, T. P.; Maloney, L.; Gogliotti, R.; Domagala, J.; Hupe, D. The in vitro ejection of zinc from human immunodeficiency virus (HIV) type 1 nucleocapsid protein by disulfide benzamides with cellular anti-HIV activity. *Proc. Natl. Acad. Sci. U.S.A.* **1996**, *93*, 969−973.

(26) Turpin, J. A.; Song, Y.; Inman, J. K.; Huang, M.; Wallqvist, A.; Maynard, A.; Covell, D. G.; Rice, W. G.; Appella, E. Synthesis and biological properties of novel pyridinioalkanoyl thiolesters (PATE) as anti-HIV-1 agents that target the viral nucleocapsid protein zinc fingers. *J. Med. Chem.* **1999**, *42*, 67−86.

(27) Goel, A.; Mazur, S. J.; Fattah, R. J.; Hartman, T. L.; Turpin, J. A.; Huang, M.; Rice, W. G.; Appella, E.; Inman, J. K. Benzamide-based thiolcarbamates: a new class of HIV-1 NCp7 inhibitors. *Bioorg. Med. Chem. Lett.* **2002**, *12*, 767−770.

(28) Basrur, V.; Song, Y.; Mazur, S. J.; Higashimoto, Y.; Turpin, J. A.; Rice, W. G.; Inman, J. K.; Appella, E. Inactivation of HIV-1 nucleocapsid protein p7 by pyridinioalkanoyl thioesters. Characterization of reaction products and proposed mechanism of action. *J. Biol. Chem.* **2000**, *275*, 14890−14897.

(29) Schito, M. L.; Goel, A.; Song, Y.; Inman, J. K.; Fattah, R. J.; Rice, W. G.; Turpin, J. A.; Sher, A.; Appella, E. In vivo antiviral activity of novel human immunodeficiency virus type 1 nucleocapsid p7 zinc finger inhibitors in a transgenic murine model. *AIDS Res. Hum. Retrov.* **2003**, *19*, 91−101.

(30) Song, Y.; Goel, A.; Basrur, V.; Roberts, P. E.; Mikovits, J. A.; Inman, J. K.; Turpin, J. A.; Rice, W. G.; Appella, E. Synthesis and biological properties of amino acid amide ligand-based pyridinioalkanoyl thioesters as anti-HIV agents. *Bioorg. Med. Chem.* **2002**, *10*, 1263−1273.

(31) Srivastava, P.; Schito, M.; Fattah, R. J.; Hara, T.; Hartman, T.; Buckheit Jr, R. W.; Turpin, J. A.; Inman, J. K.; Appella, E. Optimization of unique, uncharged thioesters as inhibitors of HIV replication. *Bioorg. Med. Chem.* **2004**, *12*, 6437−6450.

(32) Davanloo, P.; Rosenberg, A. H.; Dunn, J. J.; Studier, F. W. Cloning and expression of the gene for bacteriophage T7 RNA polymerase. *Proc. Natl. Acad. Sci. U.S.A.* **1984**, *81*, 2035−2039.

(33) Piotto, M.; Saudek, V.; Sklenar, V. Gradient-tailored excitation for single-quantum NMR spectroscopy of aqueous solutions. *J. Biomol. NMR* **1992**, *2*, 661−665.

(34) Kay, L. E.; Keifer, P.; Saarinen, T. Pure absorption gradient enhanced heteronuclear single quantum correlation spectroscopy with improved sensitivity. *J. Am. Chem. Soc.* **1992**, *114*, 10663.

(35) Altieri, A. S.; Hinton, D. P.; Byrd, R. A. Association of biomolecular systems via pulsed field gradient NMR self-diffusion measurements. *J. Am. Chem. Soc.* **1995**, *117*, 7566−7567.

(36) Delaglio, F.; Grzesiek, S.; Vuister, G. W.; Zhu, G.; Pfeifer, J.; Bax, A. NMRPipe: a multidimensional spectral processing system based on UNIX pipes. *J. Biomol. NMR* **1995**, *6*, 277−293.

(37) Garrett, D. S.; Powers, R.; Gronenborn, A. M.; Clore, G. M. A common sense approach to peak picking in two-, three-, and four-dimensional spectra using automatic computer analysis of contour diagrams. *J. Magn. Reson.* **1991**, *95*, 214−220.

(38) Grzesiek, S.; Bax, A. An efficient experiment for sequential backbone assignment of medium-sized isotopically enriched proteins. *J. Magn. Reson.* **1992**, *99*, 201.

(39) Grzesiek, S.; Bax, A. Correlating backbone amide and side chain resonances in larger proteins by multiple relayed triple resonance NMR. *J. Am. Chem. Soc.* **1992**, *114*, 6291.

(40) Wittekind, M.; Mueller, L. HNCACB, a high-sensitivity 3D NMR experiment to correlate amide-proton and nitrogen resonances with the alpha- and beta-carbon resonances in proteins. *J. Magn. Reson. Ser. B* **1993**, *101*, 201−205.

(41) Muhandiram, D. R.; Kay, L. E. Gradient-enhanced triple-resonance three-dimensional NMR experiments with improved sensitivity. *J. Magn. Reson. Ser. B* **1994**, *103*, 203-216.

(42) Fitzgerald, D. W.; Coleman, J. E. Physicochemical properties of cloned nucleocapsid protein from HIV. Interactions with metal ions. *Biochemistry* **1991**, *30*, 5195−5201.
(43) Chen, X.; Chu, M.; Giedroc, D. P. Spectroscopic characterization of Co(II)-, Ni(II)-, and Cd(II)-substituted wild-type and non-native retroviral-type zinc finger peptides. *J. Biol. Inorg. Chem.* **2000**, *5*, 93−101.
(44) Lee, B. M.; De Guzman, R. N.; Turner, B. G.; Tjandra, N.; Summers, M. F. Dynamical behavior of the HIV-1 nucleocapsid protein. *J. Mol. Biol.* **1998**, *279*, 633−649.
(45) Magyar, J. S.; Godwin, H. A. Spectropotentiometric analysis of metal binding to structural zinc-binding sites: accounting quantitatively for pH and metal ion buffering effects. *Anal. Biochem.* **2003**, *320*, 39−54.
(46) Shubsda, M. F.; Paoletti, A. C.; Hudson, B. S.; Borer, P. N. Affinities of packaging domain loops in HIV-1 RNA for the nucleocapsid protein. *Biochemistry* **2002**, *41*, 5276−5282.
(47) De Guzman, R. N.; Wu, Z. R.; Stalling, C. C.; Pappalardo, L.; Borer, P. N.; Summers, M. F. Structure of the HIV-1 nucleocapsid protein bound to the SL3 psi-RNA recognition element. *Science* **1998**, *279*, 384−388.
(48) Hathout, Y.; Fabris, D.; Han, M. S.; Sowder, R. C. I.; Henderson, L. E.; Fenselau, C. Characterization of intermediates in the oxidation of zinc fingers in human immunodeficiency virus type 1 nucleocapsid protein p7. *Drug Metab. Dispos.* **1996**, *24*, 6.
(49) Chertova, E. N.; Kane, B. P.; McGrath, C.; Johnson, D. G.; Sowder, R. C., 2nd; Arthur, L. O.; Henderson, L. E. Probing the topography of HIV-1 nucleocapsid protein with the alkylating agent *N*-ethylmaleimide. *Biochemistry* **1998**, *37*, 17890−17897.
(50) South, T. L.; Blake, P. R.; Hare, D. R.; Summers, M. F. C-terminal retroviral-type zinc finger domain from the HIV-1 nucleocapsid protein is structurally similar to the N-terminal zinc finger domain. *Biochemistry* **1991**, *30*, 6342−6349.
(51) Maynard, A. T.; Huang, M.; Rice, W. G.; Covell, D. G. Reactivity of the HIV-1 nucleocapsid protein p7 zinc finger domains from the perspective of density-functional theory. *Proc. Natl. Acad. Sci. U.S.A.* **1998**, *95*, 11578−11583.
(52) Amarasinghe, G. K.; De Guzman, R. N.; Turner, R. B.; Chancellor, K. J.; Wu, Z. R.; Summers, M. F. NMR structure of the HIV-1 nucleocapsid protein bound to stem-loop SL2 of the psi-RNA packaging signal. Implications for genome recognition. *J. Mol. Biol.* **2000**, *301*, 491−511.
(53) Goebel, F. D.; Hemmer, R.; Schmit, J. C.; Bogner, J. R.; de Clercq, E.; Witvrouw, M.; Pannecouque, C.; Valeyev, R.; Vandevelde, M.; Margery, H.; Tassignon, J. P. Phase I/II dose escalation and randomized withdrawal study with add-on azodicarbonamide in patients failing on current antiretroviral therapy. *AIDS* **2001**, *15*, 33−45.
(54) Domagala, J. M.; Gogliotti, R.; Sanchez, J. P.; Stier, M. A.; Musa, K.; Song, Y.; Loo, J.; Reily, M.; Tummino, P.; Harvey, P.; Hupe, D.; Sharmeen, L.; Mack, D.; Scholten, J.; Saunders: J.; McQuade, T. 2, 2′-Dithiobisbenzamides and 2-benzisothiazolones, two new classes of antiretroviral agents: SAR and mechanistic considerations. *Drug Des. Discovery* **1997**, *15*, 49−61.
(55) Tummino, P. J.; Harvey, P. J.; McQuade, T.; Domagala, J.; Gogliotti, R.; Sanchez, J.; Song, Y.; Hupe, D. The human immunodeficiency virus type 1 (HIV-1) nucleocapsid protein zinc ejection activity of disulfide benzamides and benzisothiazolones: correlation with anti-HIV and virucidal activities. *Antimicrob. Agents Chemother.* **1997**, *41*, 394−400.
(56) Phillips, L. R.; Malspeis, L.; Tubbs, E. K.; Supko, J. G. Characterization of a novel degradation product of 2,2′-dithiobis[N-isoleucylbenzamide], an inhibitor of HIV nucleocapsid protein zinc fingers. *J. Pharm. Biomed. Anal.* **2000**, *23*, 395−402.

JM0492195